DE GRUYTER
OPEN

DOI: 10.1515/aucts-2017-0005

ACTA UIVERSITATIS CIBINIENSIS – TECHNICAL SERIES
Vol. LXIX 2017

THE STRESS FIELD AT AN AXIAL ECCENTRICAL FATIGUE LOADING – INFLUENCED BY THE TEST TEMPERATURE

ROŞCA Vâlcu
Professor, Ph.D., Faculty of Mechanics/ Department of Applied Mechanics and Civil Constructions, University of Craiova, Craiova, Romania, rosca_valcu@yahoo.com

MIRIŢOIU Cosmin Mihai
Assistant, Ph.D, Faculty of Mechanics/ Department of Applied Mechanics and Civil Constructions, University of Craiova, Craiova, Romania, miritoiucosmin@yahoo.com

Abstract: *By applying a cyclic eccentrically tensile loading, oscillatory positive, determines at the crack peak that exist in a plate specimen CT type a compound loading of bending with tensile. The aim of the study is to analyze the equivalent stress variation σ, when the working temperature varies, namely: T= 293K (+20°C), T= 253K (-20C) and T= 213K (-60°C).*

The specimens are made from a stainless steel 10TiNiCr175 type, and were loaded with the asymmetry coefficient R= 0.1. There are drawn the variation curves of stress versus the crack length variation, σ(a), versus the material durability, σ(N), and respectively versus the stress intensity factor, σ(ΔK), for the three loading temperatures.

Key words: variable loading, asymmetry factor, stress intensity factor (SIF), loading temperature, loading stress

1. Basic notions

The stress concentration in a point or in a material area may lead to the crack initiation and then to its propagation. For a body (specimen) with side notch, cyclic loaded, the crack surfaces will have a relative displacement between them, after one of the three methods of crack propagation. The most met one is the first mode – through the crack opening, its ascension is made after a perpendicular direction on the crack front side.

It in the crack peak a trirectangular axes system Vxyz is attached, figure 1, the loading forces are toward the (y) direction, and the stress state is planar determined by the stresses: σ_x, σ_y and τ_{xy}, figure 1. A parameter is defined called "stress intensity factor" marked with K, which depends simultaneously on the loading stresses and the crack geometry, proportional with the tensor $\sigma\sqrt{\pi a}$. In the Vxy plane, the polar coordinates r and θ are established, figure 1. The stresses that appear at the crack peak are determined with the relations (1), [1], [2], [4], [5], [8]:

$$\begin{cases} \sigma_x = \dfrac{K_I}{\sqrt{2\pi r}}\cos\dfrac{\theta}{2}\left(1-\sin\dfrac{\theta}{2}\sin\dfrac{3\theta}{2}\right) \\ \sigma_y = \dfrac{K_I}{\sqrt{2\pi r}}\cos\dfrac{\theta}{2}\left(1+\sin\dfrac{\theta}{2}\sin\dfrac{3\theta}{2}\right) \\ \tau_{xy} = \dfrac{K_I}{\sqrt{2\pi r}}\sin\dfrac{\theta}{2}\cos\dfrac{\theta}{2}\cos\dfrac{3\theta}{2} \end{cases} \tag{1}$$

For the planar stress state on the crack front, the principal normal stresses σ_1 are determined, respectively σ_2, [2], [6], [7], depending on σ_x, σ_y and τ_{xy}:

$$\sigma_{1,2} = \frac{\sigma_x+\sigma_y}{2} \pm \sqrt{\left(\sigma_x-\sigma_y\right)^2+4\tau_{xy}^2} \quad \text{, or [2],} \tag{2}$$

DOI: 10.1515/aucts-2017-0005

ACTA UIVERSITATIS CIBINIENSIS – TECHNICAL SERIES
Vol. LXIX 2017

$$\begin{cases} \sigma_1 = \dfrac{K_I}{\sqrt{2\pi r}} \cos\dfrac{\theta}{2}\left(1+\sin\dfrac{\theta}{2}\right) \\ \sigma_2 = \dfrac{K_I}{\sqrt{2\pi r}} \cos\dfrac{\theta}{2}\left(1-\sin\dfrac{\theta}{2}\right) \end{cases} \tag{3}$$

These stress values can be determined during a fatigue loading by establishing some iterations for **r** vector and **θ** angle, versus the crack front, figure 1.

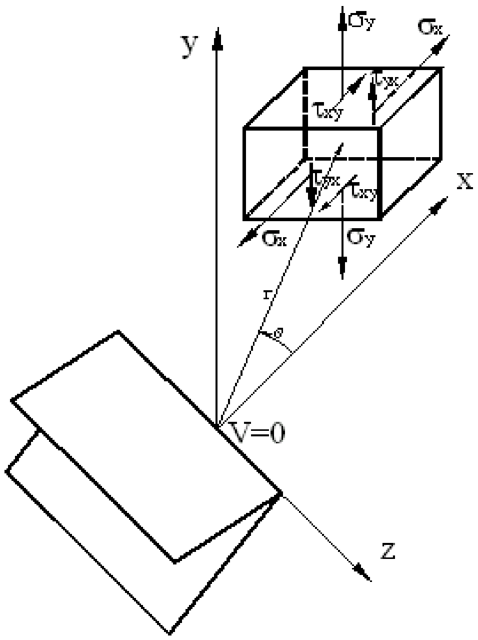

Figure 1: The stresses to top of the crack

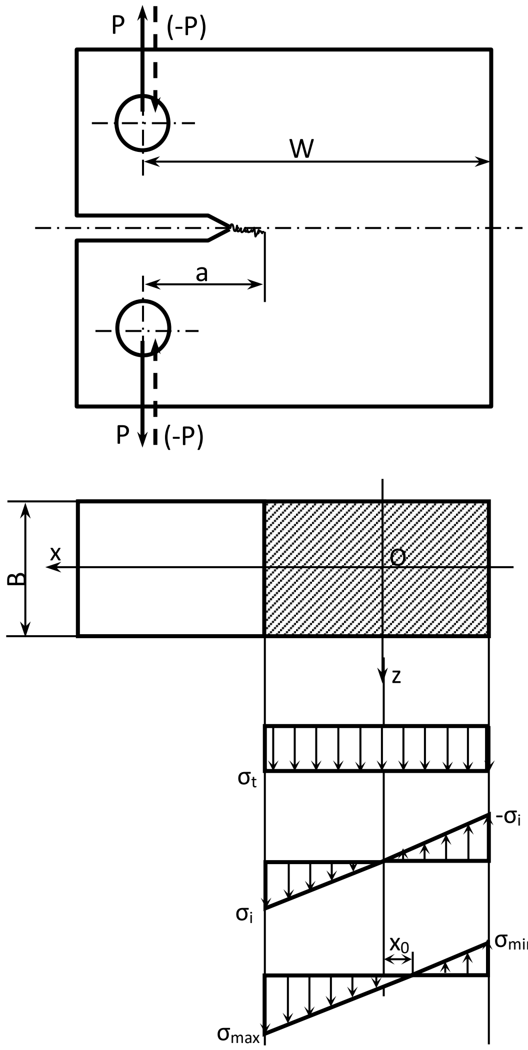

Figure 2.The specimen loading

2. Experiments and obtained data

For the experiments plate specimens were used, CT model, with side notch, figure 2, made from a stainless steel 10TiNiCr175 type, [5], [10]. These were subjected to a cyclic loading, axial – eccentrically, positive oscillatory type, with the asymmetry factor R= $\sigma_{min}/\sigma_{max}$= 0.1. Loading were made at the temperatures: T= 293K (+20°C), T= 253K (-20°C) and T= 213K (-60°C). The testing machine was a hydraulic pulsatory device Shenck type, of 30 kN, with the working frequency of 5Hz. In the first stage, the specimens were pre-cracked with an initial crack length of a_0= 2 mm, for which the corresponding number of cycles N_0 was retained. The crack length variation was followed with an optical microscope mounted on the testing machine, figure 3. For the low temperatures (253K and 213K), on the machine, a

DE GRUYTER
OPEN

DOI: 10.1515/aucts-2017-0005

ACTA UIVERSITATIS CIBINIENSIS – TECHNICAL SERIES
Vol. LXIX 2017

cryogenic chamber was mounted [5], using petroleum ether as refrigeration environment, and nitrogen (N_2L) as cooling agent. In this case, the crack length a was determined by the elastic compliance method, using an extensometer with elastic lamellae mounted on the tested specimen [5].

After the pre-crack stage, there were retained the crack length variations $\mathbf{\underline{a_i}}$, in gaps of 0.25 mm, and the corresponding number of cycles $\mathbf{N_i}$. In this way, there were highlighted primer experimental matrix data with $[a_i, N_i]$ type, necessary for the subsequent numerical processing.

For the beginning, the stress intensity factor is determined, for the cracking first mode, $\mathbf{K_I}$, with the relation (4), on the experimental data domain $\mathbf{a_i}$:

$$\Delta K = \frac{P_{\max}}{B \cdot \sqrt{W}} \cdot \frac{2+\frac{a}{W}}{\sqrt{\left(1-\frac{a}{W}\right)^3}} \cdot \left(-5{,}6 \cdot \left(\frac{a}{W}\right)^4 + 14{,}72 \cdot \left(\frac{a}{W}\right)^3 - 13{,}32 \cdot \left(\frac{a}{W}\right)^2 + 4{,}64 \cdot \left(\frac{a}{W}\right) + 0{,}886\right) \quad (5)$$

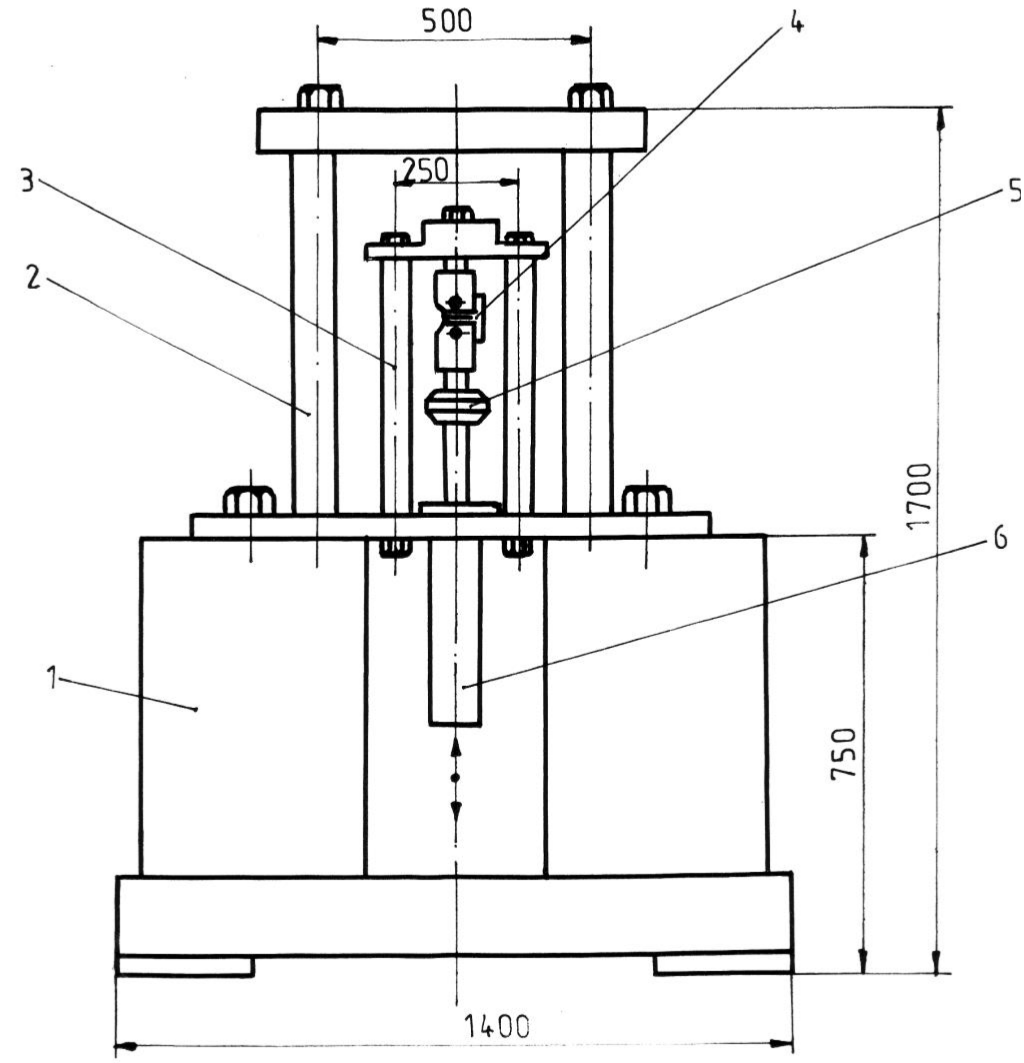

Figure 3. The testing device

The quantities from the above relation have the next specifications:
- P_{max} is the maximum loading for the chosen cycle, in this case P_{max}= 6075 N;
- B – the specimen thickness, in mm;

DE GRUYTER OPEN

DOI: 10.1515/aucts-2017-0005

ACTA UIVERSITATIS CIBINIENSIS – TECHNICAL SERIES
Vol. LXIX 2017

- W – the active specimen width, in mm, figure 2;
- a/W, is the crack normalized length, with fulfilling the condition 0.8≥ a/W ≥0.2.

3. The stress state analysis at the crack peak

For each $\mathbf{a_i}$ crack length, the stress intensity factor $\mathbf{K_I}$ will be determined. In the $[a_i, a_{i+1})$ domain, for the **r** vector but also for the **θ** angle, some iterations are imposed and the stresses at the crack peak are determined: $\boldsymbol{\sigma_x}$, $\boldsymbol{\sigma_y}$ and $\boldsymbol{\tau_{xy}}$, respectively the main stresses $\boldsymbol{\sigma_1}$ and $\boldsymbol{\sigma_2}$, with the relations (1), (2) or (3). Finally, for this gap, the maximum values of the stresses are determined: $\boldsymbol{\sigma_{x,max}}$, $\boldsymbol{\sigma_{y,max}}$ and $\boldsymbol{\sigma_{1,max}}$.

By referring to the specimen loading, we assume that it is simultaneously subjected to a tensile loading with the axial force N= P and bending toward the Vz axis with the bending moment M_i= 0,5P(W+a), figure 2. The loading stresses will be:

$$\sigma_i = \frac{M_{i,z} \cdot x}{I_z} = \frac{P \cdot \frac{W+a}{2} \cdot x}{\frac{B \cdot (W-a)^3}{12}} = \frac{6P \cdot (W+a)}{B \cdot (W-a)^3} \cdot x \tag{6}$$

$$\sigma_t = \frac{N}{A_{ef}} = \frac{P}{B \cdot (W-a)} \tag{7}$$

The resulting total stress will be the sum of the two individual ones, meaning:

$$\sigma = \sigma_t + \sigma_i = \frac{P}{W \cdot (W-a)^3} \cdot \left[(W-a)^2 + 6 \cdot (W+a) \cdot x\right] \tag{8}$$

and linearly varies, figure 2.

The axes system attached to the crack Oxyz, figure 2, has origin O mobile, being at the middle of the raw section. In this contect, at the crack peak, for x= (W-a)/2, the maximum resulting stress will be:

$$\sigma_{\max} = \sigma_c = \frac{2 \cdot P \cdot (2 \cdot W + a)}{B \cdot (W-a)^2} \tag{9}$$

On a loading cycle duration, at its superior limit, for P= P_{max}, the stress field will be:

$$\mathrm{T}_\sigma = \lfloor \sigma_{x,\max}, \sigma_{y,\max}, \sigma_{1,\max}, \sigma_{c,\max}, \rfloor \tag{10}$$

4. Graphic processing and conclusions

Based on the methodology presented above, with the obtained experimental data, respectively with the ones numerically processed the next graphics are drawn:

- the maximum stress variation: $\sigma_{x,max}$, $\sigma_{y,max}$, $\sigma_{1,max}$ and $\sigma_{c,max}$ versus the crack length variation **a**, for the temperature T= 293K, R= 0.1, figure 4;

- the maximum stress variation: $\sigma_{x,max}$, $\sigma_{y,max}$, $\sigma_{1,max}$ and $\sigma_{c,max}$ versus the stress intensity factor variation ΔK, for the temperature T= 293K and the asymmetry factor R= 0.1, figure 5;

- the same graphic types were obtained for the T= 253K temperature, figure 6 and figure 7, respectively for the T= 213K, figure 8 and figure 9;

- finally, on the same drawing, for the temperatures T= 293K, T= 253K, T=213K the resulting

DE GRUYTER
OPEN

DOI: 10.1515/aucts-2017-0005

ACTA UIVERSITATIS CIBINIENSIS – TECHNICAL SERIES
Vol. LXIX 2017

stress variation curves were drawn, for the compound loading of tensile and bending, σ_c versus the crack length variation (σ_c(a)), figure 10, respectively σ_c versus the stress intensity factor variation ($\sigma_c(\Delta K)$), figure 11.

By analyzing the graphics from figures 4…11, we can highlight some conclusions:

•- in all the figures, from 4 to 9, for the whole loading temperatures, it is observed that the stress σ_c at the compound loading is higher than the σ_y, which effectively determined the crack spread, but is inferior ,as a value, to the normal main stress σ_1. This aspect is valid for the crack length variation a but also for the stress intensity factor ΔK. For the breaking domain of stable crack propagation, followed during the tests, the normal principal stress σ_1 varies between 220 N/mm^2 and 670 N/mm^2 for T= 293K, figure 4, between 270 N/mm^2 and 650 N/mm^2 for T= 253K, figure 6, respectively between 260 N/mm^2 and 600 N/mm^2 for T= 213K, figure 8. In the same contect, the stress intensity factor ΔK is between 670 Nmm$^{-3/2}$ and 1570 Nmm$^{-3/2}$, for the temperature T= 293K, figure 5, and between 810 Nmm$^{-3/2}$ and 1590 Nmm$^{-3/2}$, for the temperature T= 253K, figure 7, and for the temperature T= 213K, ΔK varies between 800 Nmm$^{-3/2}$ and 1520 Nmm$^{-3/2}$, figure 9. We also remark that for the maximum loading stress at the crack peak σ_1 (or σ_c), but also for the stress intensity factor ΔK, there are no significant values variations for the loading temperature variation, which is not the same for the loading asymmetry factor variation R.

•- by referring to the figure 10 and figure 11 respectively, there is observed that for the same crack length variation **a**, the stress at the peak crack $\boldsymbol{\sigma_c}$ increases with the temperature decrease, figure 10, inverse aspect for the stress intensity factor, figure 11. In the same reference, for the same loading stress $\boldsymbol{\sigma_c}$, the stress intensity factor **ΔK** will increase when the environment temperature decrease.

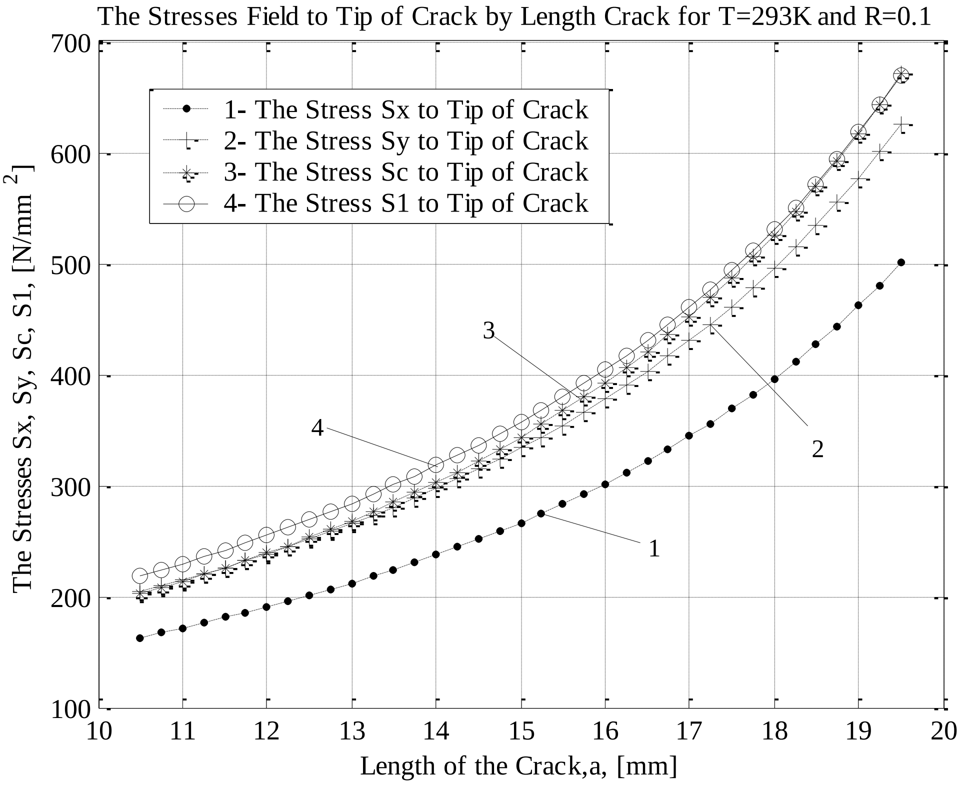

Figure 4: The stresses field to tip of crack by length crack for T=293K and R=0.1

DE GRUYTER OPEN
DOI: 10.1515/aucts-2017-0005
ACTA UIVERSITATIS CIBINIENSIS – TECHNICAL SERIES
Vol. LXIX 2017

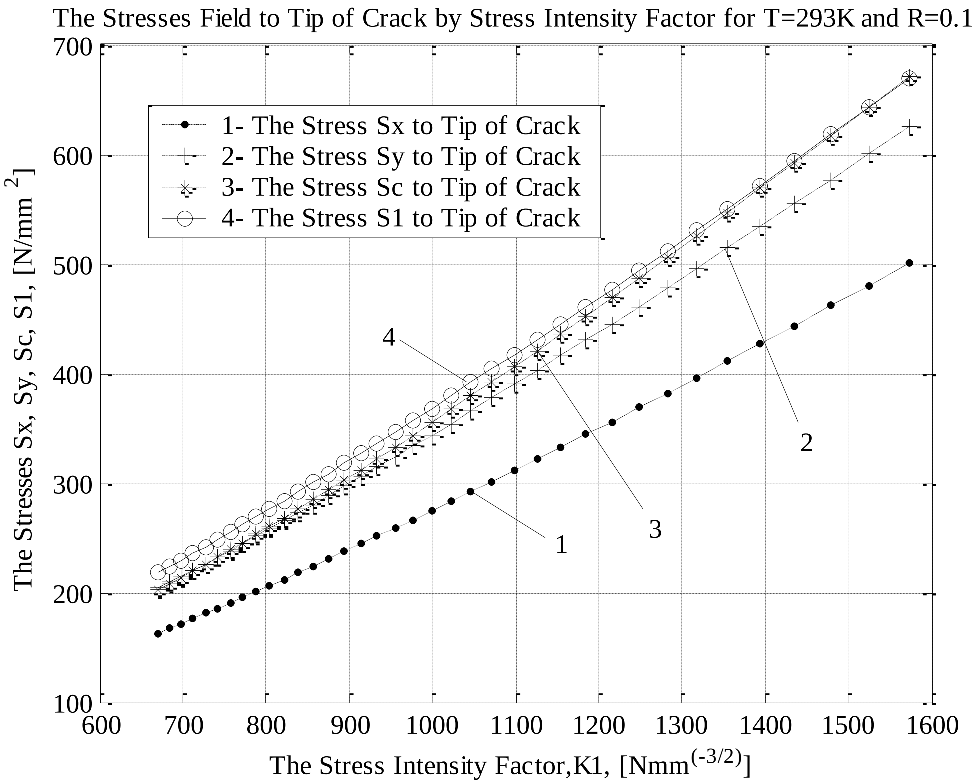

Figure 5: The stresses field to tip of crack by stress intensity factor for T=293K and R=0.1

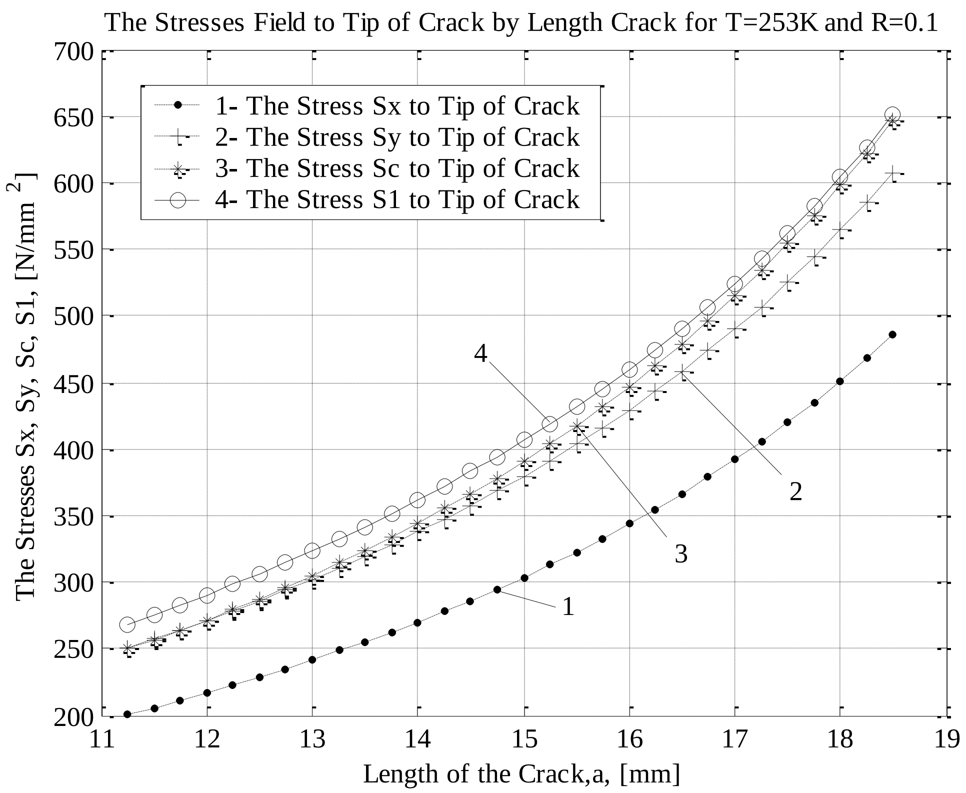

Figure 6: The stresses field to tip of crack by length crack for T=253K and R=0.1

DE GRUYTER OPEN

DOI: 10.1515/aucts-2017-0005

ACTA UIVERSITATIS CIBINIENSIS – TECHNICAL SERIES
Vol. LXIX 2017

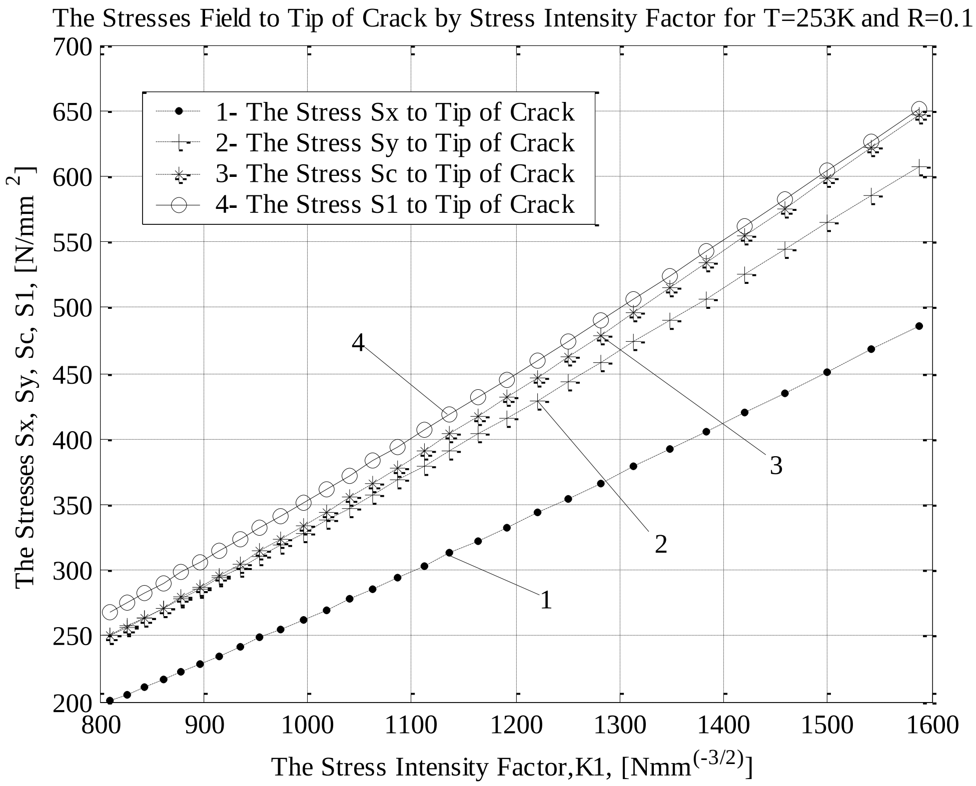

Figure 7: The stresses field to tip of crack by stress intensity factor for T=253K and R=0.1

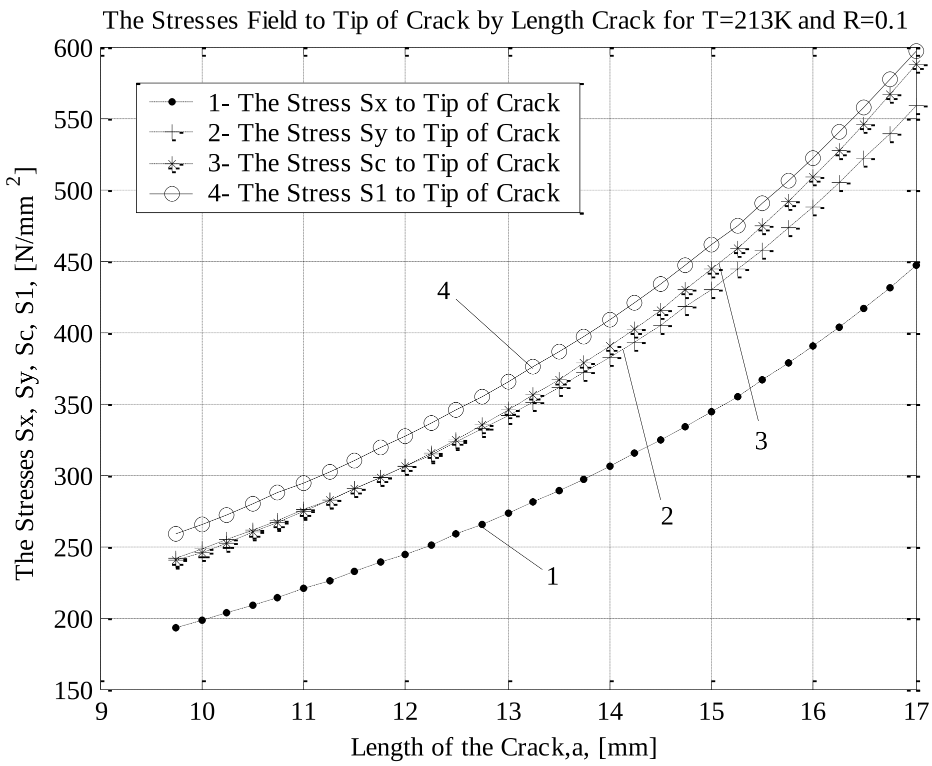

Figure 8: The stresses field to tip of crack by length crack for T=213K and R=0.1

DE GRUYTER
OPEN

DOI: 10.1515/aucts-2017-0005

ACTA UIVERSITATIS CIBINIENSIS – TECHNICAL SERIES
Vol. LXIX 2017

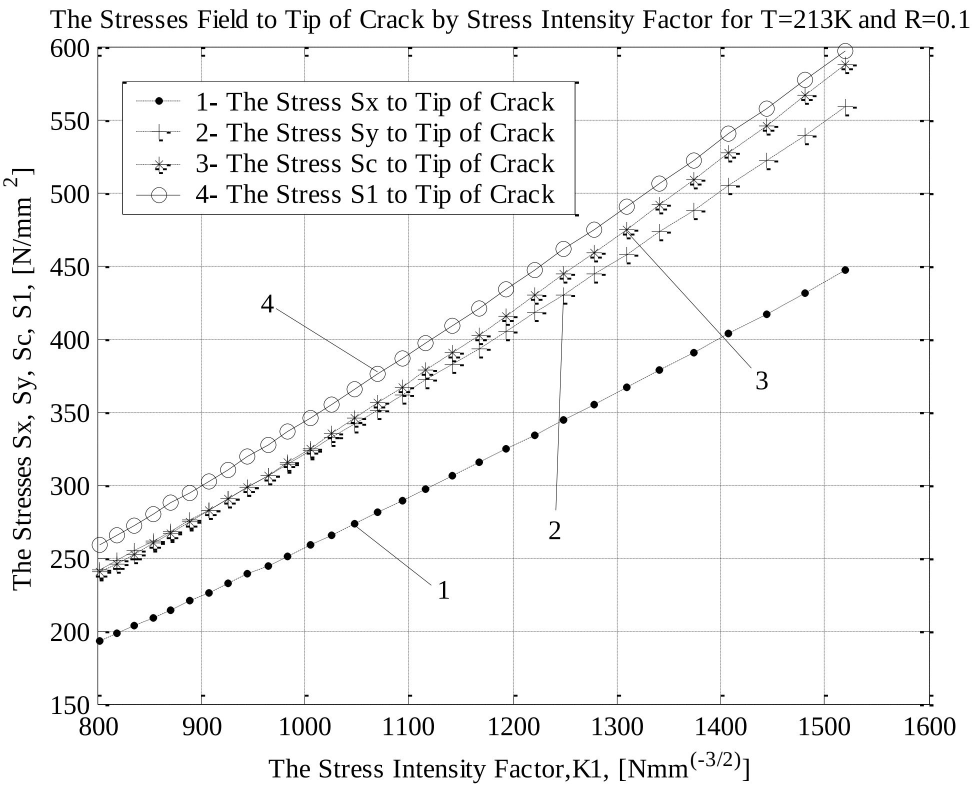

Figure 9: The stresses field to tip of crack by stress intensity factor for T=213K and R=0.1

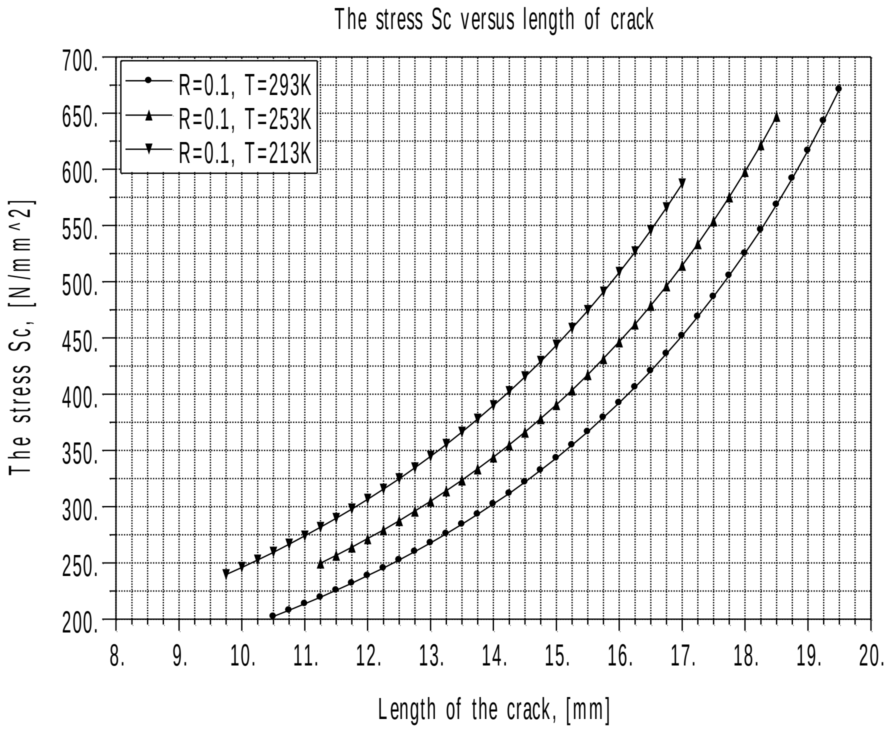

Figure 10: The stress Sc versus length of crack

DE GRUYTER
OPEN

DOI: 10.1515/aucts-2017-0005

ACTA UIVERSITATIS CIBINIENSIS – TECHNICAL SERIES
Vol. LXIX 2017

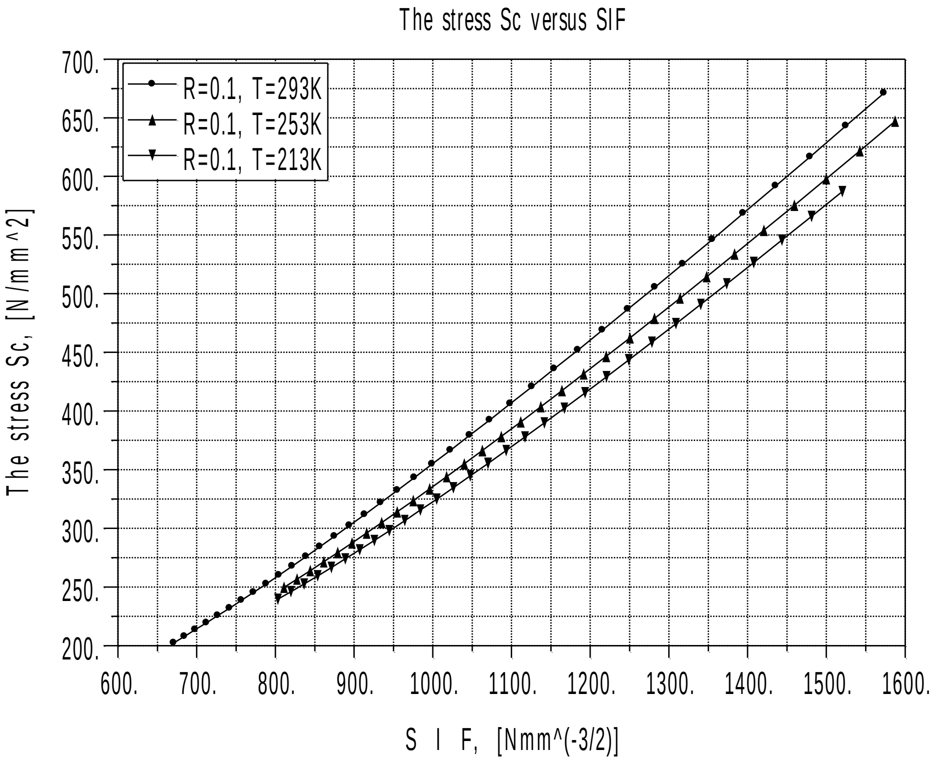

Figure 11: The stress Sc versus the stress intensity factor

5. References

1. Constantinescu, D.M., Structural integrity, University ″Politehnica″ Bucharest, (1998).
2. Dumitru, I., The basis of fatigue calculus, Eurostampa Publishing, Timisoara, (2009)
3. Mc Henry, H., I., A compliance method for crack growth studied at elevated temperatures, Journal ol Materials, 6 (4), pp. 862-873, (1971).
4. Pană, T., Pastramă, St., D., Mechanicals structures integrity, Fair Partners Publishing House, Bucharest, (2000)
5. Roşca, V., Contributions to the mono-axial fatigue study at low temperatures, Phd. Thesis, University Politehnica of Bucharest, (1997)
6. Roşca, V., The theory of elasticity applied in Strength of Materials, Curtea Veche Publishing, Bucureşti, (1997).
7. Roşca, V., The modelling of mechanical structures fracture, Universitaria Publishing, Craiova, (2008).
8. Rusu, O., Teodorescu, M., Laşcu-Simion, N., Materials fatigue, vol. 1 – Calculus basis, vol. 2 – Engineering applications, Technical Publishing House, Bucharest (1992).
9. ASTM E647-95, Standard Test Method for Measurement of Fatigue Crack Growth Rates, American National Standard.
10. Roşca, V., The variation of stress at the spike of the crack into an unoxidable steel submitted to tiredness at the temperature of 213 K, “The 10th International Symposium on Experimental Stress Analysis and Material Testing”, Vol. 1, 1-33 – 1-36, Sibiu, Romania, 21-23 October, (2004).
11. V. Roşca, C.M. Miriţoiu, The crack length gwroth – a fracture parameter in a stainless steel influenced by the temperature loading test, Applied Mechanics and Materials, 823, pp. 489-494, (2016).

